J Mol Model (2010) 16:1639–1650
DOI 10.1007/s00894-010-0676-x

ORIGINAL PAPER

Investigation on the micro-mechanisms of Al^{3+} interfering the reactivities of aspartic acid and its biological processes with Mg^{2+}

Jian Fen Fan · Liang Jun He · Jian Liu · Min Tang

Received: 23 July 2009 / Accepted: 2 February 2010 / Published online: 2 March 2010
© Springer-Verlag 2010

Abstract Density functional theory (DFT) has been applied to study the micro-mechanisms of Al^{3+} interfering the reactivities of aspartic acid (H_2asp) and its biological processes with Mg^{2+}. All the 46 stable conformers of $Hasp^-$ and 3 of asp^{2-} have been determined at the B3LYP/6-311++G** level, showing that the 7 most stable conformers of $Hasp^-$ all present a very strong and linear O–H···O H-bond between carboxyl and carboxylic acid groups with the bond energy high up to 162 kJ mol^{-1}. The reaction thermodynamics and micro-mechanism between Al^{3+} and $Hasp^-$ (or asp^{2-}) in aqueous phase have been investigated by the combined application of supramolecular model and polarizable continuum IEFPCM solvent model, firstly revealing Al^{3+} interfering in the biological processes of aspartic acid. The substitution thermodynamics and mechanisms of Mg^{2+} by Al^{3+} in the biological processes between the species of aspartic acid and Mg^{2+} in aqueous phase were probed, revealing the facile displacement of Mg^{2+} by Al^{3+}. These results may provide a reasonable mechanism of Al^{3+} biological toxicity at the microscopic level.

Keywords Al^{3+} · Aspartic acid · Mg^{2+} · B3LYP/6-311++G**

Electronic supplementary material The online version of this article (doi:10.1007/s00894-010-0676-x) contains supplementary material, which is available to authorized users.

J. F. Fan (✉) · L. J. He · J. Liu · M. Tang
College of Chemistry, Chemical Engineering and Materials Science, Soochow University,
Suzhou 215123, People's Republic of China
e-mail: jffan1305@163.com

Introduction

Many researches have demonstrated that Al^{3+} plays a strong toxic role in nervous poisoning that maybe leads to dementia, encephalopathy, memory defects, and indeed final death when the natural protective barriers of stomach and blood are overstepped. Various possible toxicity mechanisms of Al^{3+} have been speculated. Thomas [1] suggested that the strong coordinations of Al^{3+} and amino acids are possible channels of Al^{3+} toxicity. Martin [2] studied the competition courses between Al^{3+} and other metal ions, and found that the biological functions of Mg^{2+} are most likely affected, due to the fact that the exchange rate between Al^{3+} and Mg^{2+} ions is much faster than those between Al^{3+} and other metal ions. Mercero et al. [3–5] suggested that the biological toxicity of Al^{3+} comes from its competitions with other metal ions in the reactions of enzymes and proteins. The replacements of the essential metal ions (such as Mg^{2+}, Ca^{2+}, *etc*.) by Al^{3+} cause absolutely serious damages of protein functions and cell metabolism. Incorporation of Al^{3+} would lead the breakdown or chaos of the biological processes related to these essential metal ions. Mercero et al. theoretically reported that the interactions between Al^{3+} and asparagine (or glutamate) residues are much stronger than those between the non-toxic Mg^{2+} with asparagine (or glutamate) residues.

Aspartic acid (H_2asp) is one of the main amino acids building blocks of proteins. Its residues widely exist in various organisms and have important physiological functions. Aspartic acid has been widely applied in medicines, food and chemical industries. Many studies have been carried out for aspartic acid [6–11] and its residues [12–14] because of their important roles in biological processes. Edsall and Noszál et al. [8, 9] reported that aspartic acid (H_2asp) in aqueous phase can exist in multi-forms such as cationic

H_3asp^+, zwitterionic H_2asp, anionic $Hasp^-$ and asp^{2-}. They suggested that the equilibria among these species were determined by the pH of the solution. Among these species, $Hasp^-$ and asp^{2-} usually exist in the alkalescent environment.

The high-speed development of computers provides a key point for the theoretical study of the structures of amino acids and their residues. The molecular and ionic structural information of aspartic acid has a vital role in its applications in organism reactions. Ruangpornvisuti et al. [10, 11] reported the nine stable conformers of *D*–$Hasp^-$, three ones of *D*–asp^{2-}, water-added forms and their protonations at the level of B3LYP/6-31G*. Besides, the interactions between the alkali metal ions and anionic $Hasp^-$ and asp^{2-} in gas phase were investigated at the B3LYP/6-311++G** level. The most stable complex conformers of tri-coordinated Li^+–$Hasp^-$ and bicoordinated Na^+–$Hasp^-$ and K^+–$Hasp^-$ were found.

As a hydrophilic amino acid, aspartic acid has two carboxyls and one amino. One or two carboxyls may lose protons to form anionic $Hasp^-$ or asp^{2-}. Various H-bond interactions are possible between amino and carboxylic acid group (or carboxyl), resulting in complicated conformer distributions of $Hasp^-$ and asp^{2-}. Taking into account that most amino acids in organisms exist in *L*–form, the conformers and their stabilities of gaseous *L*–$Hasp^-$ and *L*–asp^{2-} are probed in this article. The coordination mechanisms and reaction thermodynamics of Al^{3+} and $Hasp^-$ (or asp^{2-}) in aqueous phase were studied, aiming to provide a possible mechanism of Al^{3+} interfering in the biological processes of aspartic acid. Finally, the competition processes between Al^{3+} and Mg^{2+} interacting with aspartic acid in aqueous phase and their thermodynamics were probed. The result reveals that Al^{3+} may probably destroy the biological processes between the essential ion Mg^{2+} and aspartic acid. This work provides some fundamental information to the study of Al^{3+} biological toxicity.

Models and computational methods

Al^{3+} interfering in the biological processes of aspartic acid

Al^{3+} is easy to hydrate, usually forming $[Al(H_2O)_6]^{3+}$ in aqueous phase [15]. Aspartic acid in organisms usually exists in the forms of $Hasp^-$ and asp^{2-} [8, 9]. This work aims at revealing the reaction thermodynamics and micro-mechanisms between Al^{3+} and aspartic acid. The following reactions were designed.

$$\left[Al(H_2O)_6\right]^{3+} + Hasp^- \rightarrow \left[Hasp - Al(H_2O)_5\right]^{2+} + H_2O \quad (1)$$

$$\left[Al(H_2O)_6\right]^{3+} + asp^{2-} \rightarrow \left[asp - Al(H_2O)_5\right]^{+} + H_2O \quad (2)$$

Martin [2] reported that the indispensable ion Mg^{2+} in organisms easily combines with aspartic acid in the following modes.

$$\left[Mg(H_2O)_6\right]^{2+} + Hasp^- \rightarrow \left[Hasp - Mg(H_2O)_5\right]^{+} + H_2O \quad (3)$$

$$\left[Mg(H_2O)_6\right]^{2+} + asp^{2-} \rightarrow asp - Mg(H_2O)_5 + H_2O \quad (4)$$

Considering the toxicity of Al^{3+} is likely ascribed to its interfering in the biological processes of Mg^{2+}, the following reactions were designed.

$$\left[Hasp - Mg(H_2O)_5\right]^{+} + \left[Al(H_2O)_6\right]^{3+} \rightarrow \left[Hasp - Al(H_2O)_5\right]^{2+} + \left[Mg(H_2O)_6\right]^{2+} \quad (5)$$

$$asp - Mg(H_2O)_5 + \left[Al(H_2O)_6\right]^{3+} \rightarrow \left[asp - Al(H_2O)_5\right]^{+} + \left[Mg(H_2O)_6\right]^{2+} \quad (6)$$

The structures and energies of all the species involved in the above reactions have been extensively studied, aiming at revealing the micro-mechanisms of Al^{3+} interfering in the reactivities of aspartic acid and its biological processes with Mg^{2+}.

The structural models of $Hasp^-$ and asp^{2-}

$Hasp^-$ can be produced by the lose of one proton from the α- or β-carboxyl of neutral aspartic acid (H_2asp), thus resulting in two possible structures. Asp^{2-} is resulted from the simultaneous lose of two protons from the α- and β-carboxyls of H_2asp. The structures and atomic numberings of $Hasp^-$ and asp^{2-} are shown in Fig. 1.

α-Carboxyl (or carboxylic acid group) and amino construct the back-bone (BB) framework, which is defined by the dihedral angles Ψ and Φ (see Fig. 1). β-Carboxyl (or carboxylic acid group) and methylene form the side-chain (SC). Its structure is determined by the dihedral angles χ_1 and χ_2 (see Fig. 1). The conformational convention for aspartic acid residues dictates nine BB (γ_D, δ_D, α_L, ε_D, β_L, ε_L, α_D, δ_L, γ_L) and nine SC (g^+g^-, a g^-, g^-g^-, g^+a, a a, g^-a, g^+g^+, a g^+, g^-g^+) conformations [12, 13]. Figure 2 illustrates the BB conformation Ramachandran map [14, 16–18] and SC conformations designated by IUPAC convention [19].

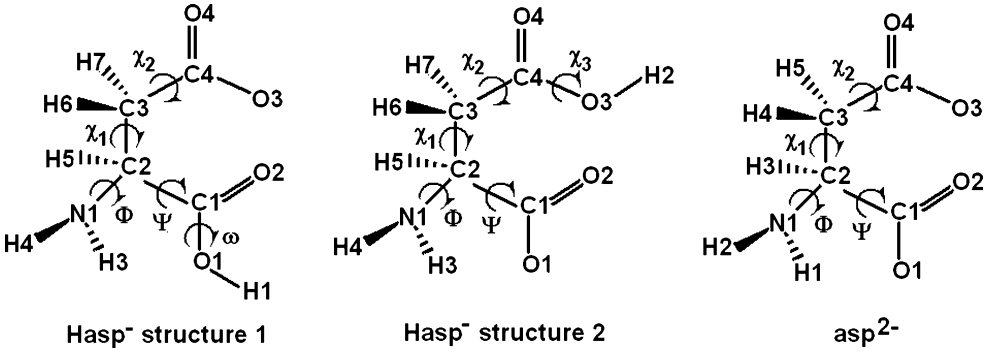

Fig. 1 Molecular structures and atomic numberings of $Hasp^-$ and asp^{2-}. Dihedral angles of $Hasp^-$ were defined as ω(H1–O1–C1–C2), Ψ(O1–C1–C2–N1), Φ(H4–N1–C2–C1), χ_1(N1–C2–C3–C4), χ_2(C2–C3–C4–O3) and χ_3(C3–C4–O3–H2), respectively. Those of asp^{2-} were defined as Ψ(O1–C1–C2–N1), Φ(H2–N1–C2–C1), χ_1(N1–C2–C3–C4) and χ_2(C2–C3–C4–O3), respectively

The dihedral angles ω(H1–O1–C1–C2) and χ_3(C3–C4–O3–H2) are used to define the arrangements of the α- and β-carboxyls in $Hasp^-$, respectively. ω=0° and 180° correspond to the *E* and *Z* arrangements of α-carboxyl, respectively. χ_3=0° and 180° are used to indicate the *endo* and *exo* arrangements of β-carboxyl, respectively [20]. Due to the *endo*/*exo* and *E*/*Z* definitions, $Hasp^-$ conformers can be categorized into four groups of $Hasp^-$-*E*, $Hasp^-$-*Z*, $Hasp^-$- *endo* and $Hasp^-$-*exo*.

The structures of $Hasp^-$ conformers were defined by the carboxyl arrangement, BB and SC conformations. For example, $Hasp^-$-*E*/α_D[g^+a] represents *E*-arrangement of α-carboxyl, α_D conformation of BB and g^+a structure of SC.

The possible conformers of $Hasp^-$ can be produced by the rotations of the chemical bonds of O1–C1, C1–C2, C2–N1, C2–C3 and C3–C4, resulting in a total of 648 (2×6×3×3×3×2) possible initial structures.

The structures of asp^{2-} conformers were defined by BB and SC conformations. For example, asp^{2-}-δ_D[g^-g^+] represents δ_D conformation of BB and g^-g^+ arrangement of SC. The possible conformers of asp^{2-} can be produced by the rotations of the chemical bonds of C1–C2, C2–N1, C2–C3 and C3–C4, resulting in a total of 81 (3×3×3×3) possible initial structures.

The structural models of metal complexes

According to the reported literatures [10, 11], metal ions easily combine with O or N atoms of amino acid residues. Based on the structures of the three most stable conformers of $Hasp^-$ and asp^{2-}, initial supramolecular geometries of $[Hasp–Al(H_2O)_5]^{2+}$ and $[asp–Al(H_2O)_5]^+$ were constructed by the incorporation of $[Al(H_2O)_5]^{3+}$, in which all the possible Al–O or Al–N bindings were attempted.

Based on the fact that Mg^{2+} and Al^{3+} have similar volumes and are easy to exchange. The initial geometries of $[Hasp–Mg(H_2O)_5]^+$ and $asp–Mg(H_2O)_5$ were constructed by the displacement of Al^{3+} by Mg^{2+} in the most stable conformers of $[Hasp–Al(H_2O)_5]^{2+}$ and $[asp–Al(H_2O)_5]^+$. Strictly speaking, the resultant structures are not absolutely certain to be the most stable structures of $[Hasp–Mg(H_2O)_5]^+$ and $asp–Mg(H_2O)_5$, respectively. However, on behalf of the similarity of Al^{3+} and Mg^{2+} ions, the simplification was made here.

Computational methods

B3LYP method [21, 22] included in Gaussian 98 suite package [23] has been applied to optimize the structures of the gaseous conformers of species involved in the reactions (1) ~ (6) with the basis set of 6-311++G**. Energy convergence precision uses the procedure default value. To minimize the errors of the DFT energies and the basis set effects, the single-point calculations at the level of MP2/aug-cc-pvdz have been performed with the B3LYP/6-311++G** optimized structures.

All the optimized structures were confirmed by frequency computations at 298 K. No imaginary frequency confirms that

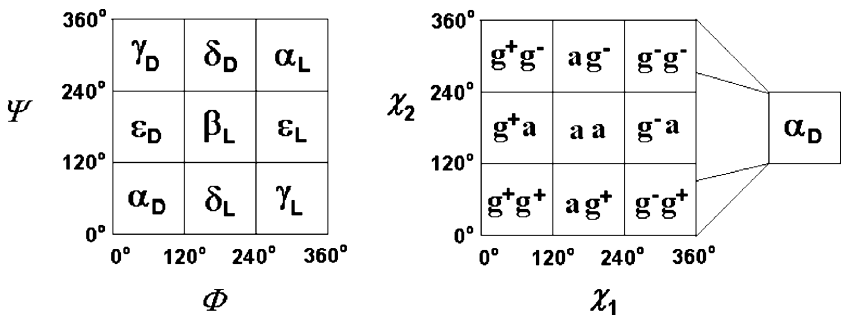

Fig. 2 Back-bone (BB) conformation Ramachandran map (left) and side-chain (SC) conformation map designated by IUPAC convention (right). The definitions of the dihedral angles Ψ, Φ, χ_1 and χ_2 can be found in Fig. 1

each structure is corresponding to a minimum on the potential energy surface.

Except the incorporations of 5 ~ 6 H_2O molecule to specify the effect of water solvent on the reactions of Al^{3+} (or Mg^{2+}) with $Hasp^-$ (or asp^{2-}) and exchange process between Al^{3+} and Mg^{2+} by using supramolecular model [see reactions (1) ~ (6)], the polarizable continuum solvent model was applied to further mimic the macro aqueous solvent effect. That is the optimized geometry of each species involved in the reactions (1) ~ (6) was further computed in aqueous phase using the IEFPCM solvent model [24] to provide the Gibbs free energy of each species. The dielectric constant ε of solvent water was chosen as 78.39. The Gibbs free energy change of each reaction was computed to study the reaction thermodynamics.

Batch operations (including the B3LYP and MP2 calculations and data processings) have been carried out to excuse us from the strenuous calculations of extensive conformational searching.

Results and discussion

$Hasp^-$ conformers and their stabilities

All the 648 possible structures of $Hasp^-$ were optimized at the B3LYP/6-311++G** level and a total of 46 stable conformers were determined. The results are presented in the supplementary Table S1, showing the relative energies of these conformers vary within 98.07 kJ mol^{-1}, and the energy gaps between the neighboring conformers are quite small. The two biggest energy gaps were found between conformers 8 and 9, and between 12 and 13, with the data of 13.80 and 14.35 kJ mol^{-1}, respectively.

Figure 3 illustrates the 12 most stable conformers of $Hasp^-$, displayed from the lowest to highest relative energies (ΔE_{MP2}) at the level of MP2/aug-cc-pvdz//B3LYP/6-311++G**. The main dihedral angle parameters and relative energies of these conformers were contained in Table 1. It should be noted that our results of *L*–$Hasp^-$ conformers are slightly different from those of *D*–$Hasp^-$ reported by Ruangpornvisuti et al. [10, 11], only nine stable conformers of *D*–$Hasp^-$ were reported there and none of them showing the special O–H···O H-bond between carboxyl and carboxylic acid groups.

As we know, H-bond interactions have important influences on the molecular stabilities of amino acids. Owing to the simultaneous presences of carboxyl, amino and carboxylic acid groups in $Hasp^-$, there are multi-types of intramolecular H-bonds in the anion. The O–H···O interaction between carboxyl and carboxylic acid groups exhibits seven-membered ring structural characteristics. The N–H···OC, N–H···OH and O–H···NH interactions between amino and α-carboxyl (or carboxylic acid group) exhibit five-membered ring structural characteristics. Such H-bonds between amino and β-carboxyl (or carboxylic acid group) adopt six-membered ring structures. Besides, the weak H-bonds C–H···OH and C–H···OC may be present between the methylene of SC moiety and α-carboxyl (or carboxylic acid group), and between the hypo-methyl of BB moiety and β-carboxyl (or carboxylic acid group). These H-bond interactions play important roles in the stabilities of 46 $Hasp^-$ conformers.

$Hasp^-$ is resulted from the lose of a proton from one of the two carboxyls of H_2asp. It is not difficult to imagine that the oxygen atoms in such carboxyl possess high electronic densities, which can easily capture neighboring protons to form H-bonds. The proton of another carboxyl is undoubtedly the best goal as for its reasonable spatial arrangement, shown in conformers 1 ~ 7. The proton of amino moiety is another possibility, shown in conformers 1, 2 and 7 ~ 12. However, due to the spatial limitation, the bond angle of the H-bond formed between amino and carboxyl (or carboxylic acid group) may not be as reasonable as that between carboxyl and carboxylic acid groups.

Figure 3 shows that the seven most stable conformers all present a very strong and linear O–H···O H-bond formed between carboxyl and carboxylic acid groups, with the very short bond length (1.35 ~ 1.49 Å) of H···O, much shorter than the ordinary ones.

In order to study the influence of such H-bond interaction on molecular stability, a supermolecule composed of the species OH^- and H_2O has been carefully studied, and the result showed that such kind of completely linear O–H···O H-bond can also be formed between these two species. One hydrogen was shared by two oxygen atoms with the distances of 1.1161 and 1.3642 Å, respectively. The O–H···O bond energy was computed as 161.72 kJ mol^{-1} using BSSE correction at the level of B3LYP/6-311++G**. As such a H-bond possesses a much shorter bond length of H···O than the ordinary ones, this H-bond interaction was suggested between covalent bond and conventional H-bond interactions.

Conformers 1 and 2 are mainly stabilized from the strong O–H···O H-bond interaction between carboxyl and carboxylic acid groups. Besides, the H-bond interaction between amino and α-carboxyl further provides molecular stability. Careful comparison of the similar structures of conformers 1 and 2 shows that the main difference is the orientation of amino moiety. The amino proton and methylene one adopt *anti*-arrangement in conformer 1, with the relatively small steric hindrance, resulting in that conformer 1 is 1.13 kJ mol^{-1} energetically favored to conformer 2.

The stabilities of conformers 3 ~ 7 are mainly contributed from the strong O–H···O H-bond interactions between

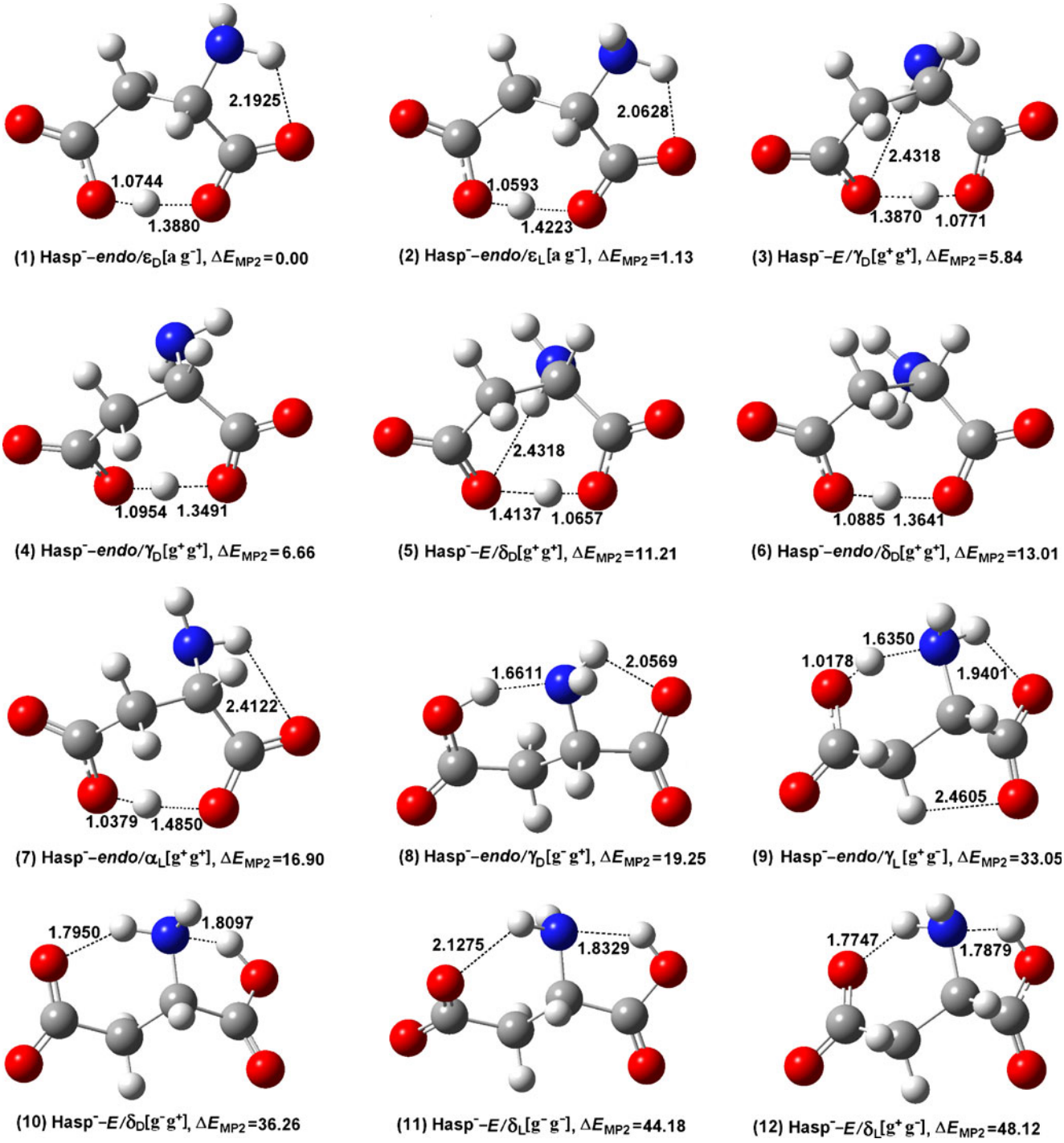

Fig. 3 The 12 most stable conformers of gaseous $Hasp^-$ obtained at the B3LYP/6-311++G** level. ΔE_{MP2} (kJ mol^{-1}) is the relative single-point energy computed at the level of MP2/aug-cc-pvdz//B3LYP/6-311++G**. The bond lengths are represented in the unit of Å

carboxyl and carboxylic acid groups. Conformer 3 possesses similar BB and SC structures as conformer 4. The mini difference is the arrangements of O–H···O H-bonds. The shared H atom locates close to the oxygen atoms of α- and β-carboxyls, with the O–H distances of 1.0771 and 1.0954 Å, respectively. Conformer 3 is 0.82 kJ mol^{-1} energetically favored to conformer 4.

Two moderate H-bond interactions exist simultaneously between the amino and carboxyl (or carboxylic acid group) in conformers 8~12. As mentioned above, the proton of amino moiety is also an aim for the carboxyl oxygen losing a proton, forming O···H–N H-bond. However, due to the spatial limitation, the bond angles of the O···H–N H-bond interactions are usually

Table 1 The main dihedral angle parameters [a] and relative energies of the 12 most stable conformers of gaseous $Hasp^-$, obtained at the level of B3LYP/6-311++G**

No.	Species [b]	ω/°	Ψ/°	Φ/°	χ_1/°	χ_2/°	χ_3/°	ΔE_{ZPE} [c] (kJ/mol)	ΔE_{MP2} [d] (kJ/mol)
1	$Hasp^-$-*endo*/ε_D[a g^-]	–	−170.0	84.9	−156.0	−44.5	0.1	0	0
2	$Hasp^-$-*endo*/ε_L[a g^-]	–	−165.5	−18.1	−157.9	−48.7	1.7	1.04	1.13
3	$Hasp^-$-*E*/γ_D[g^+g^+]	−6.0	−73.3	68.9	53.1	28.8	–	9.08	5.84
4	$Hasp^-$-*endo*/γ_D[g^+g^+]	–	−81.3	63.3	53.3	40.3	2.9	8.41	6.66
5	$Hasp^-$-*E*/δ_D[g^+g^+]	−8.4	−72.3	−173.4	46.2	35.5	–	15.34	11.21
6	$Hasp^-$-*endo*/δ_D[g^+g^+]	–	−69.2	169.9	46.7	42.8	−2.4	14.80	13.01
7	$Hasp^-$-*endo*/α_L[g^+g^+]	–	−119.6	−44.4	57.9	56.7	−5.7	20.49	16.90
8	$Hasp^-$-*endo*/γ_D[g^-g^+]	–	−17.3	23.6	−53.9	39.8	−6.8	22.78	19.25
9	$Hasp^-$-*endo*/γ_L[g^+g^-]	–	13.4	−15.4	40.7	−26.4	3.8	33.66	33.05
10	$Hasp^-$-*E*/δ_D[g^-g^+]	5.0	−17.7	151.8	−58.5	45.6	–	39.39	36.26
11	$Hasp^-$-*E*/δ_L[g^-g^-]	−2.5	15.4	−160.5	−59.2	−2.9	–	46.77	44.18
12	$Hasp^-$-*E*/δ_L[g^+g^-]	−3.3	8.9	−144.7	41.8	−13.5	–	49.59	48.12

[a] The definitions of the dihedral angles ω, Ψ, Φ, χ_1, χ_2 and χ_3 are illustrated in Fig. 1

[b] The exchange between O1 and O2 or between O3 and O4 reduces: (1) the BB of conformers 1, 2, 4, 6, 7, 8 and 9 can also be defined as α_D, γ_L, α_D, δ_L, γ_L, ε_D and ε_L, respectively (2) the SC of conformers 3, 5 and 12 can also be defined as [g^+a], and that of conformers 10 and 11 as [g^-a], respectively

[c] ΔE_{ZPE} represents the zero-point corrected energy of each conformer relative to the most stable one $Hasp^-$-*endo*/ε_D[a g^-] at the level of B3LYP/6-311++G**. The total energy and zero-point energy of $Hasp^-$-*endo*/ε_D[a g^-] are computed to be −511.968095 Hartree and 285.87 kJ mol^{-1} at this level, respectively

[d] ΔE_{MP2} stands for the single-point energy of each conformer relative to the most stable one $Hasp^-$-*endo*/ε_D[a g^-] at the level of MP2/aug-cc-pvdz//B3LYP/6-311++G**. The single-point energy of $Hasp^-$-*endo*/ε_D[a g^-] is computed to be −510.571506 Hartree at this level

not as reasonable as those of the above mentioned O–H···O ones. Also, the bond energy of O···H–N H-bond is usually smaller than that of the O–H···O one. Therefore, the conformers 8∼12 possessing two O···H–N H-bonds are much more energetically unfavored to the conformers 1 and 2. Even compared with the conformers 3∼7 only possessing one O–H···O H-bond, their stabilities are also worse. This result shows that the stabilization from the very strong O–H···O H-bond is much stronger than that from the two O···H–N H-bonds between amino and carboxyl (or carboxylic acid group) together. In fact, this can be reflected by the magnitude of the bond energy of O–H···O H-bond calculated from the supermolecule composed of OH^- and H_2O. In a word, the strong O–H···O H-bond interactions play absolutely primary roles in the stabilities of $Hasp^-$ conformers.

Except for H-bond interactions, atomic steric hindrance is also an important factor affecting molecular stability. As shown in the optimized structures of conformers 8 and 9, there is no distinct difference of the H-bond interactions between these two species. The origin of the relatively large energy gap (13.8 kJ mol^{-1}) between them is mainly contributed from the arrangement of the CH_2 of SC. Larger spatial hindrance between H atoms of CH_2 moiety with H on C_α can be found in conformer 9.

Asp^{2-} conformers and their stabilities

All 81 possible structures of asp^{2-} were optimized at the B3LYP/6-311++G** level and a total of 3 stable conformers were determined, which are *L*–enantiomers of *D*–asp^{2-} conformers provided by Ruangpornvisuti et al. [10, 11]. Figure 4 shows the optimized structures of these conformers, listed from the lowest to highest relative energies ΔE_{MP2} (kJ mol^{-1}) at the level of MP2/aug-cc-pvdz//B3LYP/6-311++G**. The main dihedral angle parameters and relative energies of these conformers were contained in Table 2.

Asp^{2-} is resulted from the simultaneous lose of two protons from the α- and β-carboxyls of H_2asp, respectively. The N–H···OC H-bond interactions are possibly formed between the amino proton and oxygen atoms of two carboxylic acid groups, shown in Fig. 4. These N–H···O H-bonds exhibit a five- or six-membered ring structural characteristic in these conformers.

The two N–H···OC H-bonds in conformer 1 possess the H···O bond lengths of 2.1937 and 2.0693 Å, and the N–H···O bond angles of 112.2° and 141.1°, respectively. The short bond length and reasonable bond angle of N–H···O between amino and β-carboxylic acid group result in the relative stability of conformer 1. The two N–H···OC H-bonds in conformer 2 have the H···O bond lengths of

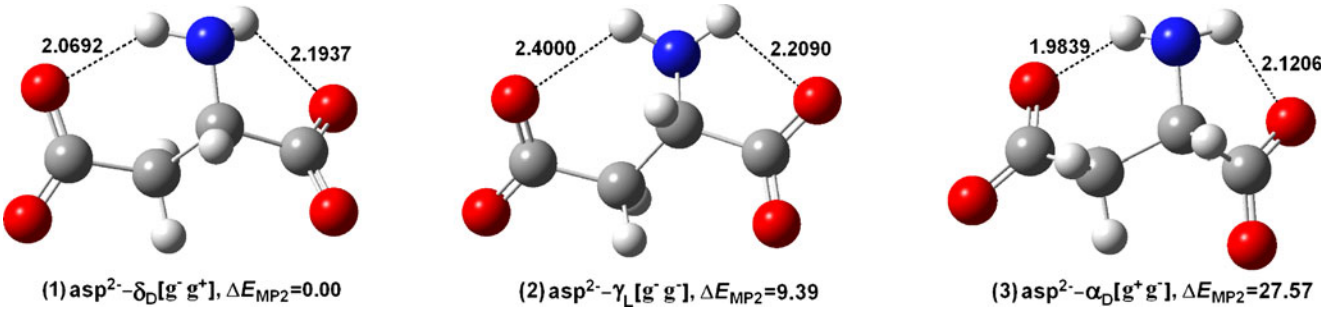

Fig. 4 The 3 stable conformers of gaseous asp^{2-} obtained at the B3LYP/6-311++G** level. ΔE_{MP2} (kJ mol^{-1}) is the relative single-point energy at the level of MP2/aug-cc-pvdz//B3LYP/6-311++G**. The bond lengths are represented in the unit of Å

2.2090 and 2.4000 Å, and the N–H···O bond angles of 108.3° and 119.5°, respectively. Obviously, the bond lengths or bond angles of these H-bonds in conformer 2 are both not as reasonable as those in conformer 1, which results in conformer 2 to be 9.39 kJ mol^{-1} energetically unfavorable to conformer 1. As for conformer 3, the H···O bond lengths of the two N–H···O H-bonds are 2.1206 and 1.9823 Å, and the N–H···O bond angles are 117.9° and 144.3°, respectively. Whether the H···O bond lengths or N–H···O bond angles show that these H-bond interactions are somewhat stronger than those in conformers 1 and 2. However, why is conformer 3 is 27.57 and 18.18 kJ mol^{-1} energetically unfavorable to conformer 1 and 2, respectively? Careful investigation on the structures of these three conformers reveals the different arrangement of the α-carbon proton relative to the two methylene protons on side chain. It can be easily found that the α-carbon proton and the methylene protons take *anti*-arrangements in conformers 1 and 2, but *syn*-arrangement in conformer 3. That is the two carboxylic acid groups in conformers 1 and 2 almost symmetrically locate at the two ends of the molecule. Such arrangement induces relatively weak atomic steric hindrance, favoring the molecular stability. Nevertheless, the α-carbon proton and two methylene protons take *syn*-arrangement in conformer 3. The significant atomic steric hindrance between these protons leads to the bending of molecular chain and simultaneous flipping back of two carboxylic acid groups. The strong steric hindrance results in conformer 3 to be the most unstable structure. Comprehensively, the H-bond interactions and atomic steric hindrances both influence the stabilities of asp^{2-} conformers together.

Al^{3+} interfering in the biological processes of aspartic acid

Among 46 stable conformers of $Hasp^{-}$, the three most stable ones were selected to study the interaction between Al^{3+} and $Hasp^{-}$ in aqueous phase. The initial supramolecular structures of $[Hasp–Al(H_2O)_5]^{2+}$ were constructed by the incorporation of $[Al(H_2O)_5]^{3+}$ to one of the three most stable conformers of $Hasp^{-}$ in all the possible binding ways and optimized at the B3LYP/6-311++G** level. Finally, 28 stable conformers of $[Hasp–Al(H_2O)_5]^{2+}$ were determined. The energy results are presented in supplementary Table S2, showing the relative energies change within 191.18 kJ mol^{-1}. Figure 5 gives the optimized structures of the four most stable conformers.

The three most stable conformers all show no direct binding between Al^{3+} and $Hasp^{-}$. However, such binding can be found in the relatively unstable conformers, such as

Table 2 The main dihedral angle parameters [a] and relative energies of the 3 stable conformers of gaseous asp^{2-}, obtained at the level of B3LYP/6-311++G**

No.	Species [b]	Ψ /°	Φ/°	χ_1 /°	χ_2 /°	ΔE_{ZPE} [c] (kJ/mol)	ΔE_{MP2} [d] (kJ/mol)
1	asp^{2-}-$\delta_D[g^- g^+]$	−32.7	149.8	−58.2	54.1	0.00	0.00
2	asp^{2-}-$\gamma_L[g^- g^-]$	26.9	−38.2	−65.1	−3.8	7.20	9.39
3	asp^{2-}-$\alpha_D[g^+ g^-]$	8.3	97.4	44.8	−15.8	23.94	27.57

[a] The definitions of the dihedral angles Ψ, Φ, χ_1 and χ_2 are illustrated in Fig. 1

[b] The exchanges between O1 and O2, and between O3 and O4 reduce: (1) the BB of conformers 1, 2 and 3 can be defined as β_L, ε_L and ε_D, respectively (2) the SC of conformers 1, 2 and 3 can be defined as $[g^- a]$, $[g^- a]$ and $[g^+ a]$, respectively

[c] ΔE_{ZPE} represents the zero-point corrected energy of each conformer relative to the most stable one asp^{2-}-$\delta_D[g^- g^+]$ at the level of B3LYP/6-311++G**. The total energy and zero-point energy of asp^{2-}-$\delta_D[g^- g^+]$ are computed to be −511.283141 Hartree and 255.31 kJ mol^{-1} at this level, respectively

[d] ΔE_{MP2} stands for the single-point energy of each conformer relative to the most stable one asp^{2-}-$\delta_D[g^- g^+]$ at the level of MP2/aug-cc-pvdz//B3LYP/6-311++G**. The single-point energy of asp^{2-}-$\delta_D[g^- g^+]$ is computed to be −509.889454 Hartree at this level

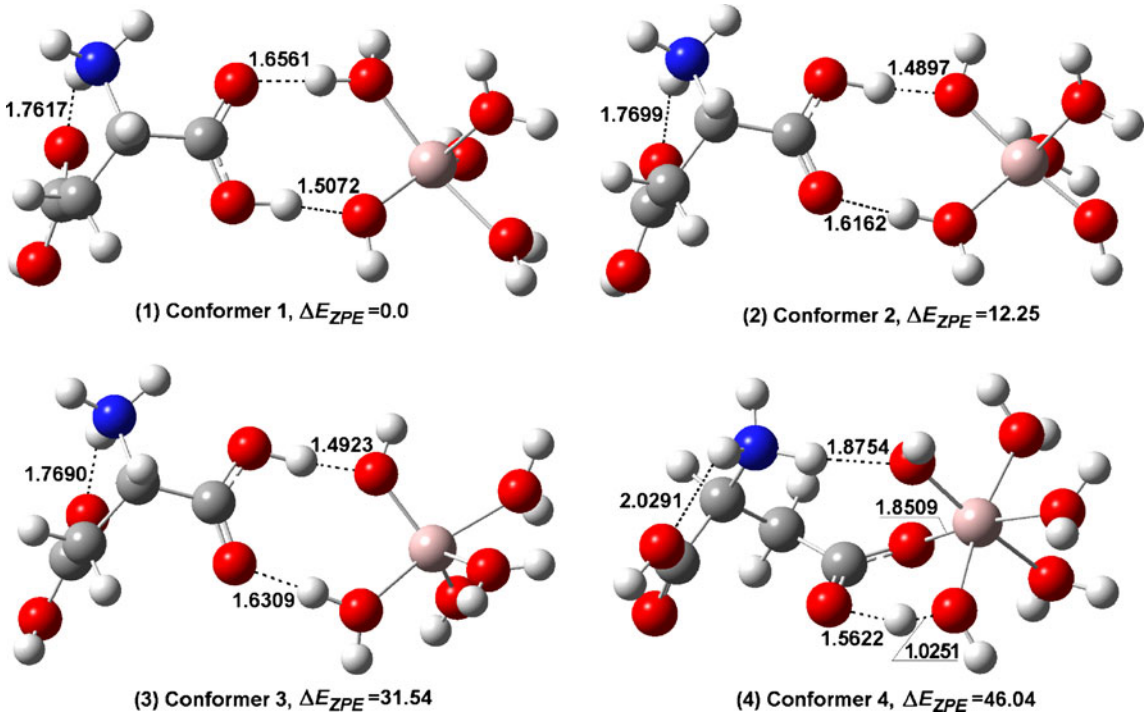

Fig. 5 The three most stable conformers of $[Hasp–Al(H_2O)_5]^{2+}$ obtained at the B3LYP/6-311++G** level. ΔE_{ZPE} (kJ mol^{-1}) represents the relative zero-point corrected energy at the level of B3LYP/6-311++G**. The bond lengths are represented in the unit of Å

conformers 4, 5 and 6, *etc*. However, these conformers possess high energies, more than 45 kJ mol^{-1} relative to conformer 1, and have low percentages according to the Boltzmann distribution principle. So it can be concluded that almost no Al–O bond can be found between Al^{3+} and $Hasp^{-}$.

NH_3^+ moiety can be observed in all four most stable conformers. Optimization processes of $[Hasp–Al(H_2O)_5]^{2+}$ structures show that the incorporation of $[Al(H_2O)_5]^{3+}$ into $Hasp^{-}$ results in the simultaneous formation of H-bonds between the surrounding H_2O molecules and carboxylic acid group, and between the H_2O molecules and carboxyl. The latter obtains a proton from a H_2O molecule and then transfers the proton to amino by forming H-bond between them. C(2)–C(3) bond rotation occurred finally. The existence of H_2O molecules makes the C–C bond rotation easy within such molecule.

Each of the three most stable conformers possesses an eight-membered ring structure containing Al–O_w bond and O_w–H_w···OC H-bond between α-carboxyl and the surrounding H_2O molecules. Such H-bond structure plays an important role on the conformational stability.

Based on the three stable conformers of asp^{2-}, the initial supramolecular structures of $[asp–Al(H_2O)_5]^+$ were constructed by the introduction of $[Al(H_2O)_5]^{3+}$ in all possible binding ways, and then optimized at the B3LYP/6-311++G** level. Finally, 38 stable conformers of $[asp–Al(H_2O)_5]^+$ were determined. The energy results are presented in the supplementary Table S3, showing the relative energies change within 393.54 kJ mol^{-1}. According to the Boltzmann principle, the distributions of conformer 5 and the following ones are very low. Figure 6 depicts the optimized structures of the four most stable conformers.

It can be found that the oxygen atoms of the carboxylic acid groups in the four most stable conformers all bind with Al^{3+}. The Al–O bond lengths between Al^{3+} and the β-carboxylic oxygen in conformers 1 and 2 possess the values of 1.8704 and 1.8712 Å, respectively. Those between Al^{3+} and the α-carboxylic oxygen in conformers 3 and 4 are 1.8624 and 1.9439 Å, respectively. The formation of the new Al–O bond is in favor of conformational stability.

As mentioned above, one of two carboxylic acid groups forms Al–O bond with $[Al(H_2O)_5]^{3+}$. Optimization processes of $[asp–Al(H_2O)_5]^+$ structures show that amino grasps a proton from a H_2O molecule first, and then transfers the proton to another carboxylic acid group by forming the H-bond between them. C(2)–C(3) bond rotation occurred finally. The existence of H_2O molecules makes the C–C bond rotation easy within such molecule, that is H_2O molecules play a lubricant role in chemical bond rotation.

The nearly coplanar six-membered ring structures containing O···H–O strong H-bond and new Al–O bond can be found in all four most stable conformers. It can be found that such H-bonds were formed between the surrounding H_2O molecules and oxygen of the carboxylic acid group coordinating with Al^{3+}. The O···H bond lengths are about

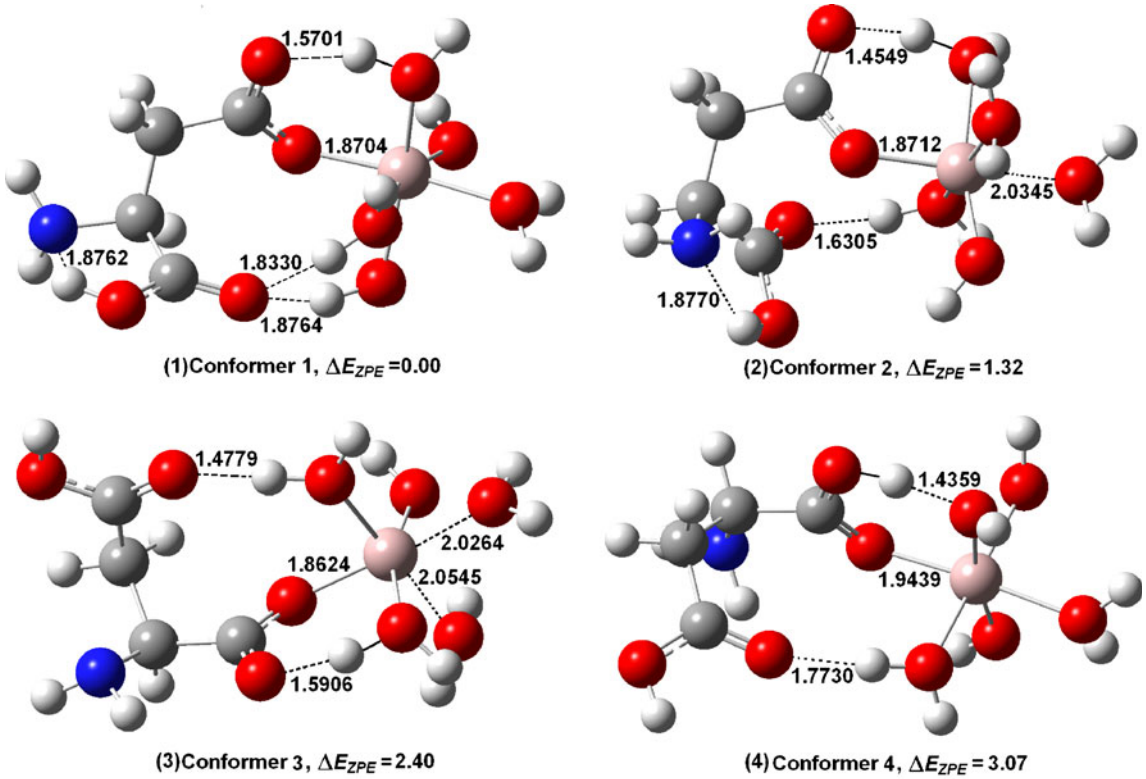

Fig. 6 The four most stable conformers of $[asp–Al(H_2O)_5]^+$ obtained at the B3LYP/6-311++G** level. ΔE_{ZPE} (kJ mol^{-1}) represents the relative zero-point corrected energy at the level of B3LYP/6-311++G**. The bond lengths are represented in the unit of Å

1.4~1.6 Å, and O···H–O bond angles are quite reasonable, about 154.0~161.1°. Careful observation reveals that the bond lengths of Al–O in the three most stable conformers are relative short (1.86~1.87 Å), and that (1.94 Å) in conformer 4 increases remarkably. Comprehensively, the stabilities of $[asp–Al(H_2O)_5]^+$ conformers 1~4 were mainly ascribed to the newly formed Al–O bond and nearly coplanar six-membered ring structure containing strong O···H–O H-bond interaction.

For conformer 1, except for the above strong H-bond interaction, the formation of the O–H···NH H-bond between α-carboxyl and amino and two strong O–H···OC H-bonds between α-carboxyl and the surrounding H_2O molecules provide the additional stability. The multiple H-bonds and their concerted effects lead conformer 1 to be the most stable one. Compared to the structure of conformer 1, only one H-bond exists between α-carboxyl and the surrounding H_2O molecules, resulting in conformer 2 to be 2.31 kJ mol^{-1} energetically unfavorable to conformer 1. There are no H-bond interactions between amino and α-carboxyl in conformers 3 and 4, and only one H-bond exists between β-carboxylic acid group and the surrounding H_2O molecule, resulting in these conformers being energetically unfavorable to conformers 1 and 2. The bond length (1.5906 Å) of H-bond between the β-carboxylic oxygen and H_2O in conformer 3 is shorter than that (1.7730 Å) in conformer 4. Conformer 3 is a little more stable than conformer 4. Their energy difference is about 1.23 kJ mol^{-1}. Comprehensively, the relative stabilities of $[asp–Al(H_2O)_5]^+$ conformers can be well explained by the formation of new Al–O bond, various H-bond interactions and their concerted effects.

Thomas [1] suggested that the strong adsorption of Al^{3+} on amino acids is a possible mechanism of Al^{3+} toxicity. The micro-mechanisms and thermodynamics of Al^{3+} reacting with aspartic acid anions $Hasp^-$ and asp^{2-} in aqueous phase, shown in the reactions (1) and (2), were studied by the combination of supramolecular and polarizable continuum IEFPCM solvent models. The results were contained in Table 3. The Gibbs free energy changes (ΔG) of the reactions (1) and (2) were calculated to be −3.77 and −101.60 kJ mol^{-1}, corrected by zero-point energy, respectively. The negative values of ΔG indicate that $Hasp^-$ and asp^{2-} can react with $[Al(H_2O)_6]^{3+}$ spontaneously in aqueous phase. A large value of the latter ΔG indicates that the reaction between Al^{3+} and asp^{2-} in aqueous phase perhaps very easily takes place. Thomas [1] suggested that the higher the binding energies of Al^{3+} and amino acids (or other biological molecules) are, the more seriously the biological processes related with such amino acids or biological molecules are blocked. These results meaningfully provide a theoretical support for the Al^{3+} interfering in the biological processes of aspartic acid.

Table 3 The Gibbs free energies of the species involved in the reactions (1) ~ (6), obtained from the combined application of the supramolecular and IEFPCM solvent models at the level of B3LYP/6-311++G**

Also listed are the total and zero-point energies derived at the same level in gas phase

[a] Each species adopts its most stable structures

Species [a]	Gibbs free energy (Hartree)	Total energy (Hartree)	Zero-point energy (kJ/mol)
$Hasp^-$	−512.059419	−511.968095	285.87
asp^{2-}	−511.57541	−511.283140	255.31
$[Hasp–Al(H_2O)_5]^{2+}$	−1136.614096	−1136.327069	640.85
$[asp–Al(H_2O)_5]^+$	−1136.167596	−1136.062960	610.94
$[Hasp–Mg(H_2O)_5]^+$	−1094.391105	−1094.290014	631.13
$asp–Mg(H_2O)_5$	−1093.939986	−1093.906425	598.95
$[Al(H_2O)_6]^{3+}$	−701.023079	−700.279725	412.72
$[Mg(H_2O)_6]^{2+}$	−658.81586	−658.508462	398.38
H_2O	−76.469134	−76.458531	55.89

Al^{3+} interfering in the biological processes of aspartic acid binding with Mg^{2+}

Mercero et al. [25] reported that Mg^{2+} is easy to combine with aspartic acid in organisms. The micro-mechanisms and thermodynamics of Mg^{2+} reacting with aspartic acid anions $Hasp^-$ and asp^{2-} in aqueous phase, shown in the reactions (3) and (4), were studied by the combination of supramolecular and polarizable continuum IEFPCM solvent models.

The optimized structures of $[Hasp–Mg(H_2O)_5]^+$ and $asp–Mg(H_2O)_5$ at the level of B3LYP/6-311++G** were shown in Fig. 7. They are quite similar to those of the most stable conformers of $[Hasp–Al(H_2O)_5]^{2+}$ and $[asp–Al(H_2O)_5]^+$, further revealing the similarity of Al^{3+} and Mg^{2+}. There are two main differences between them. First, the Mg–O bond length (2.0563 Å) in $asp–Mg(H_2O)_5$ is slightly longer than the Al–O bond one (1.8704 Å). Second, the H-bond interactions are slightly weaker for the relatively longer H-bond lengths, shown in Fig. 7. These results speculate the interactions between Mg^{2+} and the species of aspartic acid are relatively weaker than those between Al^{3+} and the species of aspartic acid in aqueous phase, which provides the possibility of Al^{3+} interfering in the biological processes of Mg^{2+} in the organisms.

Computations with IEFPCM solvent model for the optimized structures of the species involved in the reactions (3) and (4) show that the Gibbs free energy changes ΔG of these reactions are 36.72 and −48.01 kJ mol^{-1}, corrected by zero-point energy, respectively. This result indicates that Mg^{2+} can not react spontaneously with $Hasp^-$ and mainly coordinates with dianion asp^{2-} in aqueous phase. The ΔG of the reaction (4) is much small than that of the reaction (2), implying that the coordination between Mg^{2+} and asp^{2-} is probably much weaker than that between $Al^{3+}$and asp^{2-}, which provides the possibility of Al^{3+} interfering in the biological processes of aspartic acid binding with Mg^{2+}.

Much faster exchange rate between Al^{3+} and Mg^{2+} ions than those between Al^{3+} and other metal ions results in the possibility of the biological functions of indispensable Mg^{2+} being most likely affected by Al^{3+} [2]. The possible toxicity of Al^{3+} is ascribed to its interfering in Mg^{2+} biological processes [25]. In order to study the interfering mechanism of Al^{3+} to the biological processes of aspartic acid binding with Mg^{2+} in aqueous phase, the micro-mechanisms and thermodynamics of the reactions (5) and (6) were studied by the combination of supramolecular and polarizable continuum IEFPCM solvent models. Although the former computations

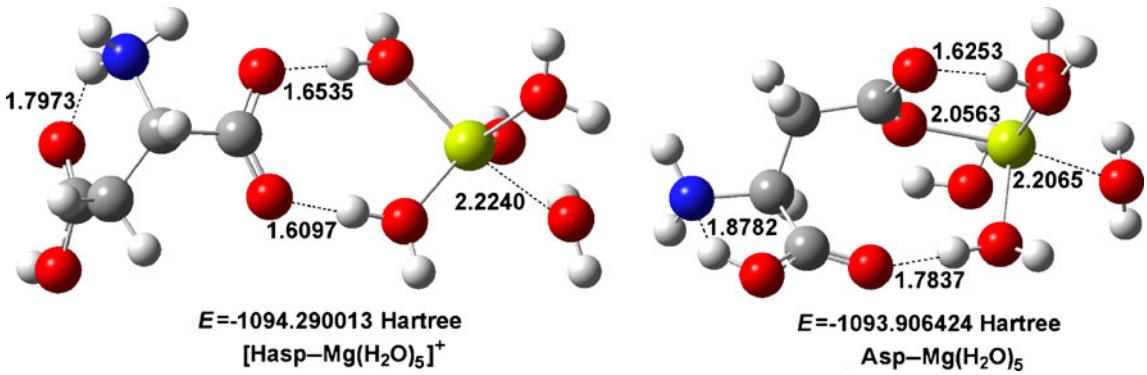

Fig. 7 The stable conformers of $[Hasp–Mg(H_2O)_5]^+$ and $asp–Mg(H_2O)_5$ at the level of B3LYP/6-311++G**. The bond lengths are represented in the unit of Å

show that the reaction between Mg^{2+} and $Hasp^{-}$ in aqueous phase cannot take place spontaneously, our simple computational model does not simulate the actual reaction conditions such as the presence of enzymes. Therefore, the study of Al^{3+} interfering the biological processes of aspartic acid binding with Mg^{2+} was carried out under the possible coordinations between Mg^{2+} and $Hasp^{-}$ or asp^{2-}.

With the data in Table 3, the Gibbs free energy changes (ΔG) of the reactions (5) and (6) are computed to be −46.03 and −55.89 kJ mol^{-1}, corrected by zero-point energy, respectively. The negative values of ΔG indicate that $[Hasp–Mg(H_2O)_5]^{+}$ and $asp–Mg(H_2O)_5$ can react with $[Al(H_2O)_6]^{3+}$ spontaneously in aqueous phase. This result shed a light on the possibility of Al^{3+} replacement of Mg^{2+} in coordination biological processes with aspartic acid. Thus, it can be concluded that Al^{3+} easily interferes the normal biological processes of Mg^{2+} and aspartic acid.

Finally, it must be noted that the above results were derived based on the simply designed reactions (1) ~ (6). In fact, the actual reactions are much more complicated in organisms. The results in this study provided a possible micro-mechanism of Al^{3+} toxicity.

Conclusions

The micro-mechanisms of Al^{3+} coordinating with the species ($Hasp^{-}$ and asp^{2-}) of aspartic acid and interfering in the biological processes between Mg^{2+} and these species in aqueous phase have been probed using density functional theory (DFT). The main achievements are shown as the followings.

(1) The 46 stable conformers of $Hasp^{-}$ and 3 of asp^{2-} have been obtained. The results show that the 7 most stable conformers of $Hasp^{-}$ present a very strong and nearly linear O–H···O H-bond with the bond energy high up to 162 kJ mol^{-1}. H-bond interactions and the atomic steric hindrances both affect the stabilities of $Hasp^{-}$ and asp^{2-} conformers.

(2) The 28 stable conformers of $[Hasp–Al(H_2O)_5]^{2+}$ have been determined. No $Al–O_{Hasp}$ bonds were found between Al^{3+} and $Hasp^{-}$. H-bond interactions play important roles on the conformational stabilities.

(3) The 38 stable conformers of $[asp–Al(H_2O)_5]^{+}$ have been determined, showing that the conformational stabilities were primarily ascribed to the newly formed $Al–O_{asp}$ bond (about 1.87~1.95 Å) and all kinds of H-bonds, especially the strong and linear O···H–O H-bond formed between carboxylic acid group and the surrounding H_2O.

(4) Calculation results of the Gibbs free energy changes showed that the reactions of $[Al(H_2O)_6]^{3+}$ and asp^{2-} (or $Hasp^{-}$) can take place spontaneously in aqueous phase, firstly providing theoretical support for Al^{3+} entering the organism interfering in the biological processes of aspartic acid. Furthermore, the results show that the replacement of Al^{3+} for Mg^{2+} in the reactions of Mg^{2+} and $Hasp^{-}$ (or asp^{2-}) can also process spontaneously, firstly providing theoretical support for Al^{3+} interfering in the biological processes of Mg^{2+} coordinating with aspartic acid, revealing the possible mechanism of Al^{3+} biological toxicity at the microcosmic level.

References

1. Thomas WS (2001) Coord Chem Rev 665:219–221. doi:10.1016/S0010-8545(01)0362-9
2. Martin RB (1994) Acc Chem Res 27:204–210. doi:10.1021/ar00043a004
3. Mercero JM, Fowler JE, Ugalde JM (1998) J Phys Chem A 102:7006–7012. doi:10.1021/jp981146b
4. Mercero JM, Fowler JE, Ugalde JM (2000) J Phys Chem A 104:7053–7060. doi:10.1021/jp992415g
5. Mercero JM, Matxain JM, Rezabal E, Lopez X, Ugalde JM (2004) Int J Quantum Chem 98:409–424. doi:10.1002/qua.20075
6. Flaig R, Koritsanszky T, Zobel D, Luger P (1998) J Am Chem Soc 120:2227–2238. doi:10.1021/ja972620e
7. Noszál B, Sándor P (1989) Anal Chem 61:2631–2637. doi:10.1021/ac00198a009
8. Edsall JT, Blanchard MH (1933) J Am Chem Soc 55:2337–2353. doi:10.1021/ja01333a019
9. Noszál B (1986) J Phys Chem 90:6345–6349. doi:10.1021/j100281a056
10. Sang-aroon W, Ruangpornvisuti V (2008) J Mol Graphics Modell 26:982–990. doi:10.1016/ j.jmgm.2007.08.004
11. Sang-aroon W, Ruangpornvisuti V (2007) J Mol Graphics Modell 26:342–351. doi:10.1016/j.jmgm.2007.01.001
12. Láng A, Füzéry AK, Beke T, Hudáky P, Perczel A (2004) J Mol Struct THEOCHEM 675:163–175. doi:10.1016/j.theochem.2003.12.047
13. Siodłak D, Broda MA, Rzeszotarska B (2004) J Mol Struct THEOCHEM 668:75–85. doi:10.1016/j.theochem.2003.10.018
14. Masman MF, Amaya MG, Rodríguez AM, Suvire FD, Chasse GA, Farkas O, Perczel A, Enriz RD (2001) J Mol Struct THEOCHEM 543:203–222. doi:10.1016/S0166-1280(01)00353-0
15. Lubin MI, Bylaska EJ, Weare JH (2000) Chem Phys Lett 322:447–453. doi:10.1016/S0009-2614(00)00434-6
16. Tarditi M, Klipfel MW, Rodriguez AM, Suvire FD, Chasse GA, Farkas O, Perczel A, Enriz RD (2001) J Mol Struct THEOCHEM 545:29–47. doi:10.1016/ S0166-1280(01)00352-9
17. Barroso MN, Cerutti ES, Rodríguez AM, Jáuregui EA, Farkas O, Perczel A, Enriz RD (2001) J Mol Struct THEOCHEM 548:21–37. doi:10.1016/S0166-1280(01)00355-4
18. Chakrabarti P, Pal D (2001) Prog Biophys Mol Biol 76:1–102
19. IUPAC-IUB Comm on Biochem Nomenclature (1970) Biochemistry 9:3471–3479
20. Sang-aroon W, Ruangpornvisuti V (2006) J Mol Struct THEOCHEM 758:181–187. doi:10.1016/j.theochem.2005.10.036
21. Becke AD (1988) Phys Rev A 38:3098–3100. doi:10.1103/PhysRevA.38.3098
22. Lee C, Yang W, Parr RG (1988) Phys Rev B 37:785–789. doi:10.1103/PhysRevB.37.785
23. Frisch MJ, Trucks GW, Schlegel HB, Scuseria GE, Robb MA, Cheeseman JR, Zakrzewski VG, Montgomery JAJr, Stratmann RE, Burant C, Dapprich S, Millam JM, Daniels JD, Kudin KN, Strain MC, Farkas O, Tomasi J, Barone V, Cossi M,

Cammi R, Mennucci B, Pomelli C, Adamo C, Clifford S, Ochterski J, Petersson GA, Ayala PY, Cui Q, Morokuma K, Rega N, Salvador P, Dannenberg JJ, Malick DK, Rabuck AD, Raghavachari K, Foresman JB, Cioslowski J, Ortiz JV, Baboul AG, Stefanov BB, Liu G, Liashenko A, Piskorz P, Komaromi I, Gomperts R, Martin RL, Fox DJ, Keith T, Al-Laham MA, Peng CY, Nanayakkara A, Challacombe M, Gill PMW, Johnson B, Chen W, Wong MW, Andres JL, Gonzalez C, Head-Gordon M, Replogle ES, Pople JA (2001) Gaussian 98, Revision A.11.2. Gaussian Inc, Pittsburgh, PA

24. Mennucci B, Cancès E, Tomasi J (1997) J Phys Chem B 101:10506–10517. doi:10.1021/jp971959k
25. Rezabal E, Mercero JM, Lopez X, Ugalde JM (2006) J Inorg Biochem 100:374–384. doi:10.1016/j.jinorgbio.2005.12.007